Research Square

Preprints are preliminary reports that have not undergone peer review.
They should not be considered conclusive, used to inform clinical practice,
or referenced by the media as validated information.

A noncanonical PLP-dependent enzyme catalyzes β-serine biosynthesis in the edeine antibiotic pathway

Gerard Wright

wrightge@mcmaster.ca

McMaster University https://orcid.org/0000-0002-9129-7131

Andrea Benediktsdottir

McMaster University

Haley Zubyk

McMaster University

Kalinka Koteva

McMaster University https://orcid.org/0000-0002-6446-9567

Erica Muscat

McMaster University

Brandon White

Brock University

Jacob Walsh

McMaster University https://orcid.org/0000-0003-4466-635X

Erin Westman

McMaster University

Travis Dudding

Brock University https://orcid.org/0000-0002-2239-0818

Sara Andres

McMaster University https://orcid.org/0000-0002-4795-2856

Article

Keywords:

Posted Date: October 29th, 2026

DOI: https://doi.org/10.21203/rs.3.rs-11078883/v1

License: This work is licensed under a Creative Commons Attribution 4.0 International License.
Read Full License

Additional Declarations: There is **NO** Competing Interest.

Abstract

PLP-dependent enzymes constitute one of the largest and most versatile enzyme families, yet few pathways for β-amino acid biosynthesis have been defined. Here we identify and characterize EdeM, a noncanonical PLP-dependent enzyme in the edeine biosynthetic pathway that generates enantiomerically pure D-β-serine through an unprecedented intramolecular rearrangement. We present crystal structures of EdeM alongside isotopic labeling and computational studies that reveal a migration of the α-carbon to the β-position. Unlike canonical aminotransferase mechanisms, which proceed through a hydrolysis-dependent step, reactions in $H_2{}^{18}O$ exclude hydrolysis, and experiments with $^{13}CO_2$ show that the carboxyl group derived from L-serine is retained without exchange with bulk CO_2. Deuterium labeling further identifies the hydrogen transfers involved. Together, these data support a 1,2-migration mechanism consistent with all experimental observations, revealing a previously unrecognized PLP-dependent rearrangement pathway. EdeM thus expands the catalytic repertoire of PLP enzymes and provides the first enzymatic route to D-β-serine.

Introduction

Microorganisms synthesize a broad array of structurally diverse metabolites, including β-amino acids, that contribute to the biological potency, stability, and protease resistance of numerous natural products. In contrast to α-amino acids, which bear the amino group on the α-carbon, β-amino acids are defined by amino substitution at the β-carbon, a feature that underpins their distinct physicochemical and bioactive properties[1, 2]. Despite their relative rarity, β-amino acids are key components of several antibiotics and bioactive peptides[3], yet their biosynthetic origins remain incompletely understood. One of the best characterized enzymatic routes to β-amino acids involves aminomutases that convert α-amino acids into their β-isomers. Two mechanistically distinct classes have been characterized: 4-methylideneimidazole-5-one (MIO)-dependent enzymes, which catalyze elimination–addition reactions on aromatic substrates[4], and radical aminomutases, which employ pyridoxal phosphate together with an additional cofactor such as adenosylcobalamin or radical S-adenosyl-L-methionine (SAM) to mediate 1,2-amino group rearrangements[2, 3]. However, these mechanisms do not account for the full diversity of β-amino acid structures found in natural products, indicating that additional, uncharacterized biosynthetic strategies must exist.

The closely related peptide antibiotics edeines (A, B, D and F, Fig. 1a), produced by the *Brevibacillus brevis* Vm4 strain, target the 30S ribosomal subunit in both prokaryotes and eukaryotes, inhibiting translation through a recently characterized mechanism that disrupts the mRNA trajectory through the E-site[5]. This activity is mediated in part by distinctive features of edeine, notably its incorporation of several β-amino acids. Edeines, therefore, exemplify the structural complexity and functional importance of β-amino acid-containing natural product[6, 7]. Encoded by a 45.1-kb biosynthetic gene cluster (BGC) (Fig. 1b), edeines incorporate four nonproteinogenic amino acids, including three β-amino acids: β-tyrosine/β-phenylalanine, β-serine, and 2,3-diaminopropionic acid (DAPA), as well as the gamma-amino

acid 2,6-diamino-7-hydroxyazelaic acid (DAHAA) into their linear pentapeptide scaffold[8]. While the biosynthesis of β-tyrosine/β-phenylalanine and DAPA has been elucidated in related system[9–11], the origin of β-serine is unknown, and the biosynthetic pathway to DAHAA remain poorly understood.

Here, we report the identification and functional analysis of EdeM, a noncanonical pyridoxal 5'-phosphate (PLP)-dependent enzyme in the edeine biosynthetic pathway that catalyzes the formation of D-β-serine. PLP is a versatile cofactor that catalyzes a wide range of amino acid transformations by stabilizing carbanionic intermediates, including transamination, epimerization, decarboxylation, retro-aldol chemistry, Claisen condensation, and β- or γ-elimination/substitution reactions[12, 13]. However, PLP-dependent reactions that reorganize the carbon skeleton of an amino acid to generate a β-amino acid are rare and poorly defined, with known examples typically requiring additional cofactors or proceeding through a radical mechanism[14]. Based on our observations, we hypothesized that EdeM catalyzes a noncanonical PLP-dependent transformation converting L-serine to D-β-serine. Through isotopic labeling, enzymatic reconstitution, and mechanistic analysis, we reveal that EdeM catalyzes an unusual carbon-skeleton rearrangement converting L-serine into β-serine, requiring only PLP as cofactor. This discovery establishes the first enzymatic route for β-serine biosynthesis and uncovers a new mode of PLP-mediated amino acid transformation.

Results

Analysis of Edeine biosynthesis

Edeine is assembled by a hybrid non-ribosomal peptide synthetase (NRPS) encoded by a specialized BGC containing several large and multi-modular *ede* proteins. To elucidate the architectural logic of this assembly line, we profiled the substrate specificities of the NRPS adenylation domains using two complementary predictive platforms: NRPS Transformer[15] and PARAS/PARASECT[16], which were run in parallel, followed by domain mapping using antiSMASH. Although these analyses did not fully resolve the biosynthetic sequence, they supported assignments for most of the amino acid-incorporating modules. EdeI is assigned to glycine activation, EdeK to DAPA, and EdeN to β-tyrosine (Fig. 1a-b), (Supplementary Table 1). EdeP is predicted to activate asparagine and contains an epimerization domain, making it a strong candidate for incorporation of the D-asparagine-containing prodrug motif identified in preedeine[17] (Supplementary Fig. 1). The enzymatic basis for DAHAA biosynthesis remains mechanistically unresolved. Based on the predicted domain architecture, we hypothesize that DAHAA is assembled on the hybrid NRPS–PKS machinery from smaller amino acid-derived precursors, with EdeJ and EdeL as possible contributors. Isotope-feeding experiments and targeted gene deletions will be required to determine the precursor origins and establish the precise biosynthetic sequence. As previously established by our group, the BGC also encodes the N-acetyltransferase EdeQ, which confers self-resistance by acetylating the free amino group of the internal DAPA residue, thereby inactivating edeine and protecting the producing organism[8].

To investigate the biosynthesis of β-serine in edeine, we prioritized candidate genes within the edeine BGC by excluding those associated with established β-tyrosine/phenylalanine and DAPA pathways. A homology search identified EdeM, a pyridoxal 5'-phosphate (PLP)-dependent enzyme sharing 71% sequence identity with aspartate aminotransferase (AAT), as a strong candidate (Fig. 1c). AAT is a fold-type I, class I aminotransferase known for catalyzing the reversible conversion of aspartate and α-ketoglutarate into glutamate and oxaloacetate (Fig. 1d)[18]. Following overexpression and purification, X-ray crystallography confirmed that EdeM adopts a canonical fold-type I transaminase architecture. Despite this structural conservation, biochemical characterization showed an unexpected catalytic activity.

EdeM converts L-serine to D-β-serine without additional substrates

The close structural similarity to canonical aminotransferases suggested that EdeM may utilize PLP-dependent amino group transfer chemistry. We therefore hypothesized that EdeM may similarly mediate amino group transfer, using L-serine as the donor and 2-hydroxy-3-oxopropionic acid as the acceptor to generate β-serine. To investigate this activity, *edeM* was cloned from the edeine biosynthetic gene cluster, heterologously expressed in *E. coli*, and purified to homogeneity for *in vitro* assays. Initial endpoint assays revealed that EdeM catalyzed the formation of β-serine in the presence of L-serine without the addition of an exogenous amino group acceptor. This result suggests that EdeM performs a noncanonical PLP-dependent reaction distinct from the typical transamination mechanism employed by AAT and other aminotransferases, which require both amino donor and acceptor substrates. To assess substrate specificity, EdeM activity was tested against a panel of alternative amino acids (L-alanine, L-valine, L-leucine, L-methionine, L-asparagine, L-aspartate, L-threonine, L-cysteine, L-phenylalanine, L-tryptophan, and D-serine). No detectable product formation was observed with any of the tested substrates, indicating that EdeM exhibits stringent selectivity for L-serine.

EdeM exhibits an absorbance at 388 nm, which matches the absorbance maximum seen for free PLP in solution (Supplementary Fig. 41), suggesting that PLP exists in an unbound state in the active site of EdeM. Steady-state kinetic analysis of EdeM was performed using an HPLC-based assay. The enzyme exhibited a Michaelis constant (K_M) of 1.75 mM and a turnover number (k_{cat}) of 0.06 s^{-1}, resulting in a catalytic efficiency (k_{cat}/K_M) of 3.43×10^1 $M^{-1}s^{-1}$ (Supplementary Fig. 44). These values are consistent with those reported for PLP-dependent enzymes involved in secondary metabolism, which typically operate at lower catalytic rates than their primary metabolic counterparts[19]. EdeM's kinetic profile resembles that of AAT, despite its mechanistic divergence from canonical transaminases[20].

Structural analysis of EdeM reveals conservation with canonical transaminases

We determined high-resolution crystal structures of both apo-EdeM (PDB ID: 38JZ, 1.7 Å, Supplementary Fig. 3) and EdeM bound to reduced PLP (PDB ID: 38RJ, 2.3 Å, Fig. 2a-b). Because the native PLP-bound intermediate was difficult to crystallize, we generated a stable mimic by reducing PLP with $NaBH_3CN$ and covalently linking the reduced PLP to the catalytic lysine; we refer to this adduct as PLR. Structural comparison with *E. coli* AAT (PDB ID: 1ARG)[21], a canonical fold-type I, class I transaminase, shows that EdeM adopts a conserved dimeric architecture typical of this enzyme family. Like AAT, EdeM forms a homodimer of 387 residues (44.2 kDa) and displays the domain organization characteristic of class I PLP enzymes: a large PLP-binding domain, a flexible small domain involved in substrate binding, and a short N-terminal strand that stabilizes the dimer interface (Fig. 2a and Supplementary Fig. 3). Comparison of the apo and PLR-bound structures captures this flexibility directly. Whole-protein alignment gives an RMSD of 1.85 Å (Supplementary Fig. 3), driven largely by inward movement of the small domain toward the active site, with the domain itself shifting by up to 4.9 Å and adjacent loop regions moving 2.1 Å. This closed conformation in the EdeM-PLR structure mirrors the open-to-closed transition described for AAT. Consistent with a closed, substrate-bound state, an acetate ion is co-crystallized in the active site, mimicking the carboxylate group of an amino acid substrate. Despite these conformational changes, the active site geometry is well conserved: alignment of the EdeM and AAT active sites yields an RMSD of 0.84 Å. Key catalytic residues are retained, including K258 (Schiff base formation), D202 (PLP ring protonation), R365 (substrate carboxylate binding), and N175, Y205, and R243 (PLP phosphate and pyridine ring stabilization) (Fig. 2b). One notable substitution is AAT's PLP-interacting W140 for Y126 in EdeM, which still supports similar π-stacking with PLP. This conservation of catalytic geometry, despite EdeM's divergent substrate profile, suggests that its unusual reactivity arises from differences elsewhere in the active site rather than from the core PLP-binding chemistry.

Conserved tyrosine residues in EdeM are essential for catalysis

To identify residues critical for the EdeM mechanism, we compared EdeM with a homologous enzyme (EdeM-GE) encoded in the biosynthetic gene cluster of the RNA polymerase-targeting antibiotic GE23077, which also incorporates D-β-serine (Fig. 2c). Several fold-type I PLP-dependent enzymes were selected as references for conserved active-site residues in aminotransferases and decarboxylases, including tyrosine aminotransferase (TAT), L-threonine-O-3-phosphate decarboxylase (TPDC), aspartate aminotransferase (AAT), histidinol-phosphate aminotransferase, glutamate decarboxylase, 2,2-dialkylglycine decarboxylase, and ornithine decarboxylase (Fig. 2d). As expected, EdeM-GE was the most structurally similar to EdeM, with a Z-score of 46.3 and 56% sequence identity, and both enzymes contained four conserved active-site tyrosine residues (Y126, Y205, Y240, Y320) (Fig. 2e,f), a feature unique among the PLP enzymes analyzed. Mutating these tyrosine residues to phenylalanine in EdeM revealed that Y205F and Y240F mutants were catalytically inactive, while Y126F and Y320F exhibited > 47-fold reductions in catalytic efficiency (Fig. 2g). Active site tyrosines in AATs often help orient substrates via hydrogen bonding and serve as a major determinant of specificity. However, in most canonical AATs, these tyrosines are not strictly essential for catalysis, and their mutation has been shown to reduce efficiency but does not abolish activity[22]. In contrast, our results demonstrate that

EdeM exhibits a unique dependence on tyrosine for activity, highlighting a mechanistic distinction from canonical aminotransferases.

Mechanistic analysis suggests an atypical single-substrate transamination

Extensive evidence demonstrates that transaminases operate through a conserved reversible ping-pong, bi-bi mechanism that includes two half-reactions, which is supported by characteristic initial-velocity kinetics and the accumulation of the pyridoxamine phosphate (PMP)-bound enzyme intermediate[23]. In fold type I PLP-dependent enzymes, catalysis proceeds via transaldimination between enzyme-bound PLP and the incoming amino acid substrate, followed by formation of a quinonoid intermediate and rearrangement to a ketimine, which undergoes hydrolysis to release the corresponding α-keto acid while generating PMP[23, 24] (Fig. 3). In canonical transaminations, a second α-keto acid substrate subsequently reacts with PMP through the reverse sequence, regenerating PLP and producing a new amino acid[25]. EdeM's strict requirement for only L-serine to generate D-β-serine ruled out a classical ping-pong mechanism, but we hypothesized a modified mechanism in which the predicted first product of a transaminase-like mechanism, 3-hydroxy-2-oxopropanoic acid (**5**), could undergo keto-enol tautomerization to form 2-hydroxy-3-oxopropanoic acid (**8**). This tautomer could then serve as an internal amino group acceptor, enabling completion of the reaction without a second exogenous substrate (Fig. 3). To test this hypothesis, we used isotope tracing by conducting the reaction in $H_2{}^{18}O$ (Fig. 3). If hydrolysis of the ketimine intermediate (**4**) occurred, incorporation of ^{18}O into the keto-acid (**5**) carboxyl group would be expected to carry through to the final D-β-serine product. However, repeated reactions with EdeM and L-serine showed no ^{18}O enrichment in the final product, inconsistent with the formation and hydrolysis of a free α-keto acid intermediate (Fig. 3). These results indicate that EdeM does not follow the canonical ping-pong bi-bi mechanism of transamination[25]. Instead, its activity likely proceeds via a concerted or intramolecular mechanism that bypasses the need for hydrolysis and a second substrate, representing a previously uncharacterized mode of PLP enzyme catalysis.

Does EdeM catalyze a CO_2-mediated rearrangement of L-serine to D-β-serine?

Given the absence of a hydrolysis step in EdeM catalysis, we hypothesized that L-serine remains covalently tethered to the PLP cofactor throughout the reaction and undergoes rearrangement. To trace the atomic origin of the D-β-serine product, preparative-scale reactions were performed using L-serine labeled with 2-^{15}N (Fig. 4b-i), 3–$^{17/18}O$ (Fig. 4b-i*i*), 1-^{13}C (Fig. 4b-i*ii*), and 2-^{13}C (Fig. 4b-i*v*). After 1 hour of reaction, the product was derivatized with Marfey's reagent to facilitate purification. HRMS and NMR analyses revealed that the 2-^{13}C label had shifted to the β-position (3-^{13}C) in D-β-serine, whereas the 1-^{13}C label was retained (Fig. 4c). This carbon rearrangement is incompatible with the canonical two-half reaction mechanism depicted in Fig. 3, and thus these data support a rearrangement mechanism in

which the serine carboxyl group forms a new C–C bond with the side-chain hydroxyl carbon, yielding a novel α-chiral center and repositioning the amino group at the β-position.

EdeM's activity was tested in the dark and found to proceed as efficiently as in the light, indicating that photoexcitation or light-driven radical formation is not required (Supplementary Fig. 10). EdeM encodes no radical cofactors such as SAM, MIO, or iron–sulfur clusters, and *in vitro* reconstitution shows that PLP alone is sufficient for catalysis and produces an enantiomerically pure product. These observations strongly support a PLP-dependent rearrangement mechanism rather than one involving radical intermediates.

The strict dependence of EdeM on tyrosine hydroxyl groups, in contrast to canonical AATs, together with the positioning of Y240 and Y320 to engage the substrate carboxylate, suggests a role in stabilizing a CO_2-derived intermediate during catalysis. We therefore proposed a putative mechanism (Fig. 5) involving initial decarboxylation (**12**), followed by retention of the liberated CO_2 within the active site through hydrogen-bonding interactions with the key tyrosine residues Y320 and Y240 (Fig. 5). A subsequent deprotonation generates a nucleophile at the side-chain hydroxy-carbon, which attacks the sequestered CO_2 (**14**) to re-form a carboxylate at a new position on the substrate (**15**), thereby accounting for the observed carbon rearrangement. To probe the extent to which substrate-derived CO_2 can be induced to exchange with bulk CO_2, we conducted reactions under an atmosphere of isotopically labeled carbon dioxide ($^{13}CO_2$, 99.7% ^{13}C), following degassing and gas exchange to challenge retention within the active site. Under the proposed mechanism, incorporation of ^{13}C into D-β-serine should not occur, and consistent with our observations after repeated attempts, the product formed exhibited only the natural isotopic distribution with no detectable ^{13}C enrichment (Fig. 4b-v and Supplementary Fig. 7). These results show that exogenous CO_2 was not incorporated into the product during the rearrangement process, making the direct transfer of CO_2 unlikely, but not impossible. However, downstream experiments did not support this mechanism (*vide infra*).

Does EdeM convert L-serine to D-ß-serine via Favorskii-type rearrangement or a 1,2-migration mechanism?

To gain further mechanistic insights, the enzymatic reaction was performed in D_2O at a preparative scale to map hydrogens that undergo exchange during the enzymatic reaction. HRMS analysis (Supplementary Fig. 9) of the isolated product showed incorporation of two atoms of deuterium ($\Delta m/z$ = + 2 Da) into D-β-serine, and NMR analysis confirmed both were located at the β-carbon (C3) (Fig. 4e and Supplementary Fig. 37). To further probe hydrogen dynamics, we reacted EdeM with commercially available L-3,3-D_2-serine (98%), observing the loss of one deuterium atom during the reaction (Fig. 4f). These results are inconsistent with the proposed decarboxylation mechanism proposed above in Fig. 5, as that pathway would predict incorporation of only a single deuterium atom, rather than the two observed at the same carbon. To rule out substrate dimerization, a crossover experiment was performed using a 1:1 mixture of

^{15}N-L-serine and 3-^{13}C-L-serine. The resulting product showed no isotope crossover (Supplementary Fig. 8) confirming that the rearrangement occurs intramolecularly.

Based on the biochemical and isotopic labeling data, we considered two mechanistic scenarios that could account for the observed deuterium incorporation and carbon rearrangement. To distinguish between them, we performed density functional theory (DFT) calculations using active site theozyme models to evaluate the intrinsic reactivity, energetic feasibility, and relative likelihood of the proposed pathways.

The first mechanism involves a Favorskii-like rearrangement[26] (Fig. 6a-I). Proton abstraction from the hydroxyl-bearing carbon of intermediate **18** generates enamine **19**, which could attack the adjacent carboxyl carbon to promote a 3-exo-trig cyclization, consistent with the Baldwin's rules[27, 28], forming intermediate **20**. In classical Favorskii rearrangements, intramolecular cyclization generates a strained three-membered ring that can facilitate subsequent bond reorganization[26, 29]. Formation of the cyclopropanimine intermediate **20** introduces substantial ring strain and electronic destabilization, which could promote ring opening to give imine **21**. Unlike the classical Favorskii rearrangement, which proceeds through cyclopropanone or cyclopropanolate intermediates derived from α-haloketones, the proposed pathway involves a PLP-bound cyclopropanimine. Cyclopropanimines have previously been synthesized and isolated by two labs[30, 31], however, with methyl substituents rather than hydroxyl groups. We reasoned that a corresponding PLP-bound intermediate could be transiently stabilized within the enzyme active site while remaining too short-lived for experimental detection.

To evaluate the proposed Favorskii-like cyclization pathway, DFT calculations examined the proposed cyclized intermediate **20** and searched for transition states leading to its formation Although these searches did not identify a transition state connecting the reactant to **23**, geometry optimizations converged to cyclized structures closely resembling the proposed intermediate. These structures exhibit the expected cyclopropanimine-like geometry, demonstrating that a strained three-membered-ring species can be accommodated within the PLP framework when stabilized by the surrounding active-site residues. We identified a computed Favorskii-like structure 20 (Supplementary Fig. 45) stabilized by the two tyrosine residues (Y320 and Y240), together with several closely related conformations, indicating that stabilization of this species depends on specific enzyme–substrate interactions rather than on the PLP cofactor alone.

While these findings indicate that a Favorskii-like intermediate is a viable local minimum, the absence of a computationally tractable pathway for its formation prompted us to investigate a concerted 1,2-migration pathway (Fig. 6a-II) consistent with the experimental observations and accounting for both the deuterium incorporation and the carbon-skeleton rearrangement. In this pathway, rather than undergoing decarboxylation, protonation of **19** generates intermediate **22**, which is poised to undergo a facile 1,2-migration of the adjacent carboxylate group via transition state **TS-1**, with a computed Gibbs free energy of activation of only 6 kcal/mol (Fig. 6b).

The computed transition-state structure reveals an extensive hydrogen-bonding network that organizes the reacting groups and lowers the barrier for carbon migration. These interactions are preorganized by the two proximal tyrosine residues (Y320 and Y240) and are further reinforced by the quinonoid phenol cofactor within the theozyme model. In **TS-1**, the migrating carboxylate transfers with a breaking C–C bond distance of 1.9 Å and a forming C–C bond distance of 2.2 Å (Fig. 6b). The development of charge polarization along the reaction coordinate is supported by the electrostatic potential (ESP) surface and natural bond orbital (NBO) atomic charge analysis, which reveal increased negative charge density localized on the carboxylate oxygen atoms bearing natural charges of -0.706 and − 0.663. This charge buildup is stabilized by hydrogen-bonding interactions with the tyrosine residues, thereby facilitating the migration process. Formation of the resulting intermediate **23** is strongly exergonic, with an overall reaction free energy of − 30 kcal/mol. Subsequent PLP-dependent transamination of the imine intermediate would yield the corresponding D-β-serine product. Collectively, these calculations provide compelling support for the direct 1,2-carboxylate migration mechanism, for which a viable transition state and a low-energy reaction pathway were successfully identified.

Discussion

This study establishes EdeM as a mechanistically distinct PLP-dependent enzyme responsible for the biosynthesis of D-β-serine in the edeine antibiotic pathway. While structurally homologous to fold-type I aminotransferases, EdeM diverges fundamentally in its catalytic mechanism, enabling a single-substrate rearrangement of L-serine to D-β-serine without requiring an external amino acceptor or a hydrolysis step. Through a systematic and extensive process of excluding hydrolysis, decarboxylation, substrate-dimerization and radical-based mechanisms, our experiments, including isotopic labeling, $H_2{}^{18}O$ incorporation, $^{13}CO_2$ probing, and deuterium tracing, collectively support a polar, intramolecular rearrangement mechanism. Notably, the carboxyl group of L-serine is retained and repositioned from the α- to the β-carbon, forming a new C–C bond and a novel chiral center.

The reaction proceeds with strict enantioselectivity, consistently yielding enantiomerically pure D-β-serine. This stereochemical control, combined with the absence of crossover between isotopically labeled substrates, argues against mechanisms involving free radicals or intermolecular exchange and instead supports an intramolecular rearrangement within the enzyme active site. DFT calculations further favor a low-barrier 1,2-carboxylate migration over a Favorskii-type cyclization, with the active site hydrogen-bonding network, particularly Y320 and Y240, stabilizing charge development during the rearrangement. Mutational analysis identifies four conserved tyrosines in the active site, two of which (Y205 and Y240) are essential for catalysis, highlighting the critical role of their hydroxyl groups, a feature that is nonessential in canonical aminotransferases. Structurally, EdeM retains the fold-type I aminotransferase architecture, demonstrating that small modifications within a well-conserved scaffold can enable entirely new chemical transformations.

Beyond mechanistic novelty, the ability of EdeM to generate enantioselectively pure D-β-serine has potential practical relevance. The pharmaceutical industry has long sought biocatalytic routes to

enantiomerically pure β-amino acids due to their value as building blocks in peptide therapeutics and small-molecule drugs. By defining a naturally evolved, single-enzyme route to D-β-serine, this work provides a blueprint for enzymatic production processes that could be scaled or engineered for synthetic applications. Overall, these data define EdeM as the first known PLP-dependent enzyme to catalyze an intramolecular rearrangement of an amino acid to yield a β-amino acid, representing a novel enzymatic strategy for β-serine biosynthesis. This work expands our understanding of the catalytic plasticity of PLP-dependent enzymes and provides a foundation for the mechanistic dissection of a previously unknown class of amino acid–modifying biocatalysts. A question for future studies is how the D-β-serine produced by EdeM is incorporated into edeine. Analysis of hydrolyzed edeine B by Marfey's derivatization and HRMS identified L-β-serine in the final product, indicating that the stereochemistry generated by EdeM is altered prior to peptide incorporation. This finding raises the possibility of a yet unidentified epimerase acting downstream of EdeM and highlights an additional step in the pathway that remains to be characterized. Identifying this enzyme and defining when and where epimerization occurs will be important for establishing the complete biosynthetic route to edeine.

Methods

Molecular Cloning

Genomic DNA from *Brevibacillus brevis* Vm4 was isolated and used as the DNA template to amplify *edeM* (GenBank ID: AHH86047.1) using Phusion DNA polymerase (Thermo Scientific) according to the manufacturer's instructions. Oligonucleotide primers encoding NdeI and HindIII restriction sites were used to amplify the gene and allow insertion into the pET28a overexpression vector. The PCR product was purified and digested with the respective restriction enzymes (Thermo Scientific FastDigest Enzymes) and ligated into similarly digested pET28a before transformation into *Escherichia coli* TOP10 chemically competent cells. EdeM mutants (K40A, K235A, Y126F, Y205F, Y240F, Y320F) were prepared using site-directed mutagenesis. The sequences of all constructs were verified by Sanger sequencing (MOBIX Lab, McMaster University) before transformation into *E. coli* BL21 (DE3).

Overexpression and Purification

Overexpression strains were grown in 1L of autoinduction media (autoclaved 1% yeast extract and 2% tryptone in ddH_2O supplemented with 0.2% 1M $MgSO_4$, 4% 50X LAC [25 g glycerol, 2.5 g glucose, 10 g lactose per 100 mL ddH_2O], 5% 20X NPSC [53.5 g NH_4Cl, 32.23 g Na_2SO_4, 66 g KH_2PO_4, 71 g Na_2HPO_4 per 1 L ddH_2O], 0.1% trace elements [1 g $FeSO_4 \times 7H_2O$, 8.8 g $ZnSO_4 \times 7H_2O$, 0.4 g $CuSO_4 \times 7H_2O$, 0.15 g $MnSO_4 \times 4H_2O$, 0.1 g $Na_2B_4O_7 \times 10H_2O$, 0.05 g $(NH_4)_6MO_7O_{24} \times 4H_2O$ in 1 L ddH_2O]) supplemented with kanamycin (50 mg/mL) and one 250 mg vitamin B6 tablet (Jamieson) as a source of PLP precursor for 3 days at 25°C and 180 rpm. Cells were harvested by centrifugation at 6,400 × g, 4°C, and resuspended in lysis buffer (25 mM HEPES [pH 7.5], 300 mM NaCl, and 10 mM imidazole). Resuspended cells were lysed using a continuous cell disrupter (Constant Systems Limited, Daventry UK) at 20,000 psi, 4°C in the

presence of lysozyme (Bioshop), deoxyribonuclease (Sigma Aldrich), and Pierce EDTA-free protease inhibitor tablets (Thermo Scientific). Whole-cell lysate was centrifuged at 30,000 × g to remove cell debris before incubating clarified lysate with 1 mL of Ni-NTA resin (Qiagen) equilibrated in lysis buffer for 30 minutes on ice. The lysate-resin slurry was then loaded onto an Econo-Pac chromatography column (1.5 x 12 cm) (Bio-Rad) with a 20 mL bed volume, and the resin was washed with wash buffer (25 mM HEPES [pH 7.5], 300 mM NaCl, and 25 mM imidazole). Proteins were eluted using elution buffer (25 mM HEPES [pH 7.5], 300 mM NaCl, and 250 mM imidazole) before overnight dialysis at 4°C against 2 L of dialysis buffer per protein (25 mM HEPES [pH 7.5], 300 mM NaCl, 0.25 mM tris(2-carboxyethyl)phosphine (TCEP)). Sample purity was assessed by running the elution on a 12% SDS-PAGE and visualizing the gel with Coomassie Blue R-250 staining solution before concentrating via a centrifugal filter column (Amicon Ultra-15, 30,000 NMWL) and storage at 4°C. All samples prepared using this method were used in downstream assays. Samples used for native EdeM crystallization were further purified by anion exchange (HiTrap Q HP 5 mL, GE Healthcare) on the FPLC system (ÄKTA-explorer 100 Air; GE Healthcare) using a low to high salt gradient (low salt buffer: 25 mM HEPES [pH 7.5], 50 mM NaCl, high salt buffer: 25 mM HEPES [pH 7.5], 300 mM NaCl). Samples containing EdeM were detected at 280 nm and analyzed using SDS-PAGE before concentration and storage at 4°C. For the selenomethionine incorporated EdeM, pET28a:edeM was transformed into E. coli B834 before expression in M9 minimal media supplemented with amino acids (no methionine) and L-selenomethionine. Media was inoculated with a starter culture (1:250) and grown to OD_{600} = 0.5 at 37°C, 250 rpm before inducing expression with 1 mM isopropyl β-D-1-thiogalactopyranoside (IPTG) for 20 h at 16°C. The same purification methods were followed as those used for native EdeM crystallization.

In vitro Assay Conditions

EdeM assays were carried out in 100 uL reactions containing 100 mM HEPES [pH 7.5], 150 mM NaCl, 1 mM L-serine, 30 mM of EdeM, and 30 mM of PLP. Reactions were incubated at 25°C for 1 h before pre-column derivatization. Derivatization reactions contained 10 uL enzyme reaction, 10 uL 1 M $NaHCO_3$, and 50 uL of 1% Marfey's reagent (N_{α}-(2,4-dinitro-5-fluorophenyl)-L-valinamide) solubilized in acetone. These reactions were incubated at 40°C for 1 h before being terminated with 10 uL of 1 M HCl, followed by dilution with 420 uL MeOH.

High-performance Liquid Chromatography (HPLC)

Derivatized enzyme reactions were filtered, and 15 µL was injected on to an Agilent Eclipse XDB-C8 column (3.5 µm, 2.1 x 100 mm) and analyzed by HPLC (Agilent 1260 Infinity, Agilent Technologies). The run method was optimized to separate the L-serine starting material and D-β-serine product (rt = 16 min and 17 min). The HPLC separation was performed at 0.4 ml/min using the following gradient: 0 min, 10% B; 1 min, 20% B; 20 min, 30% B; 21 min, 90% B; 22 min, 10% B; 28 min, 10% B. Solvents A and B were H_2O 0.1% formic acid and CH_3CN, respectively. Absorbance was monitored at 340 nm.

Steady-State Kinetics

Steady-state kinetics parameters of EdeM were determined using a non-continuous HPLC-based assay, following the in vitro assay conditions and HPLC analysis methods previously described. Standard curves for L-serine and D-β-serine were developed in the absence of the enzyme. The area under the curve (AUC) for each concentration of L-serine and D-β-serine was plotted using GraphPad Prism. Simple linear regression was applied to establish the equation of the line, which was then used to calculate the concentration of D-β-serine produced by EdeM. The enzyme was assayed across various concentrations of L-serine: 0, 0.05, 0.1, 0.25, 0.5, 1, and 2 mM, with each concentration tested in duplicate. Reactions were quenched after 15 minutes—a timeframe determined to be within the linear range of the reaction—by directly adding the sample to Marfey's derivatization reagents and initiating derivatization. The samples were subsequently analyzed by HPLC as described above. The AUC values for D-β-serine were converted to concentrations for each L-serine concentration tested. These results were analyzed using GraphPad Prism by nonlinear regression fit to the Michaelis-Menten Eq. (1).

1. $v = (k_{cat}/E_t)S/(K_m + S)$

Mass Spectrometry

Derivatized enzyme reactions were filtered, and 0.5-1 µL was injected on the Q-TOF LC/MS (Agilent Technologies 6550 iFunnel) using an Agilent Eclipse XDB-C8 column (3.5 µm, 2.1 x 100 mm). The run method was optimized to separate the L-serine starting material and D-β-serine product (Rt = 12.5 min and 13.5 min). The LC/MS was run at 0.2 ml/min using the following gradient: 0.5 min, 10% B; 1 min, 20% B; 20 min, 30% B; 21 min, 90% B; 22 min, 10% B. Solvents A and B were H_2O and ACN, respectively.

Apo-EdeM crystallization

Crystals were grown at 23°C using the hanging-drop vapour diffusion method with 1 uL of protein solution (1.83 mg/mL) combined with 1 uL of each condition from the Nextal PEGS II suite (Calibre Scientific) and 500 µL of 1.5 M ammonium sulphate in each reservoir. Crystals grew in the precipitant condition containing 0.1 M Tris [pH 8.5] and 8% PEG 8000. Crystals were not cryoprotected before flash freezing in liquid nitrogen prior to diffraction data collection. Diffraction data were collected at the McMaster Macromolecular X-ray Diffraction Facility before collecting at the Canadian Light Source (CLS) using beamline CMCF-ID[32]. Crystals had a strong diffraction signal of 2.5 Å with weak spots at 2.2–2.3 Å using the home source and an improved diffraction signal of 1.8 Å at the CLS; however, the crystal phase could not be determined. Selenomethionine derivatized EdeM (1.83 mg/mL) was then used to set up crystal trays with a matrix of the initial crystallization condition (0.1 M Tris at [pH 7.5], [pH 8.0], [pH 8.5], [pH 9.0] and 6%, 8%, 10%, 12% PEG 8000). Crystals formed in 0.1 M Tris [pH 7.5] with 10% PEG 8000 at 23°C. Crystals were not cryoprotected prior to flash freezing in liquid nitrogen before diffraction data

collection. Initial phases were determined by single-wavelength anomalous dispersion (SAD) using a selenomethionine-substituted crystal, with data collected to 2.0 Å resolution at the Se absorption peak (λ = 0.97928 Å). Initial phases were calculated using Phenix AutoSol. An initial model was built with Phenix AutoBuild. This model was subsequently used as a search model for molecular replacement with Phaser against a higher-resolution native dataset collected to 1.7 Å, and the resulting structure was refined through iterative cycles of manual rebuilding in Coot[33] and refinement in Phenix.refine[34] to a final Rwork/Rfree of 14.2/15.9. Atomic coordinates were deposited in the PDB, accession number: 38JZ.

EdeM-PLR Crystallization

EdeM sample supplemented with PLP was reduced using 1 M $NaBH_3CN$ for 1 h in the dark before washing the sample with buffer to remove the reducing agent and excess PLP. Crystals were grown at 23°C using the hanging-drop vapour diffusion method. Drops containing 1 uL of protein solution (1.83 mg/mL) and 1 uL of reservoir solution were equilibrated against 200 uL of reservoir solution using each condition from the MCSG Suites (Calibre Scientific). Crystals grew in 0.1 M MES [pH 5.5], 10% PEG 8000, and 0.2 M calcium acetate. Crystals were cryoprotected in mother liquor mixed with 25% PEG 8000 before flash-freezing prior to diffraction data collection. Diffraction data were collected at the CLS, CMCF-BM, with a diffraction signal to 2.3 Å. The structure was solved by molecular replacement using Phenix.phaser and the apo-EdeM structure. Refinement was completed using Phenix.refine[34] and coot[33]. Reduced PLP (PLR) and acetate (co-crystallized in the active site from the 0.2 M calcium acetate crystallization condition) were modelled into the Fo-Fc difference map after initial rounds of refinement, with final model refined to an Rwork/Rfree of 16.7/20.7. Atomic coordinates were deposited in the PDB, accession number: 38RJ.

Protein-ligand structure prediction model

AlphaFold 3[35] was used to predict a model for EdeM docked with cyclopropanimide intermediate **22** with an excellent score seed of pTM: 0.96, ipTM: 0.98. The docking was achieved using Protenix-v1-20250630[36] under academic license: Apache 2.0. Structures were visualized in PyMOL version 3.1.4[37].

Labelling with $^{18}OH_2$

Reactions were set up using 100 mM HEPES [pH 7.5], 150 mM NaCl, 30 mM EdeM, and 1 mM L-serine solubilized in $^{18}OH_2$ (99% ^{18}O, Sigma Aldrich), with 86% of the total volume (100 uL) comprised of pure $^{18}OH_2$. As a positive control for $^{18}OH_2$ incorporation, reactions containing the metallo-β-lactamase NDM-1[38] (1 mM) and meropenem (0.5 mM) were prepared and treated the same. Controls for both EdeM and NDM-1 reactions were prepared in H_2O. Reactions were incubated at 30°C for 1 h before derivatizing reaction contents with Marfey's reagent, as previously described. Derivatized reaction samples were

injected into the Q-TOF LC/MS (Agilent Technologies 6550 iFunnel) to detect $^{18}OH_2$ incorporation using the same method as previously described.

Labelling with $^{13}CO_2$

Reactions were set up using the standard reaction buffer and conditions as described above but in 50 uL scale and under an atmosphere of isotopically labeled carbon dioxide ($^{13}CO_2$, 99.7% ^{13}C, Sigma Aldrich), following first degassing and gas exchange several times. A series of reactions were set up with increasing amounts of CO_2 gas bubbled through the reaction, incubated at 25°C, and monitored after 1, 2 and 4 h before derivatizing reaction contents with Marfey's reagent, as previously described. Derivatized reaction samples were injected into the Q-TOF LC/MS (Agilent Technologies 6550 iFunnel) to detect ^{13}C incorporation using the same method as previously described.

Enzymatic reaction in deuterium oxide

Reactions were set up under standard enzymatic reaction conditions in D_2O (99% D, Sigma Aldrich) instead of H_2O at 1 mL scale. Control reactions in D_2O without enzyme showed no covalent deuterium exchange. Reactions were incubated at 25°C, monitored for 1 and 4 h, and left overnight before derivatizing reaction contents with Marfey's reagent, as previously described. Derivatized reaction samples were injected into the Q-TOF LC/MS to detect deuterium incorporation using the same method as previously described.

Purification and NMR analysis of the deuterated D-β-serine

The derivatized samples were lyophilized and resuspended in 3 mL of DMSO before loading 1.5 mL volume at a time onto a 50 g C8 RediSepGold column for purification via flash chromatography (CombiFlash Rf 200) at 25 mL/min using the following gradient: 1 min, 10% B; 10 min, 30% B; 30 min, 50% B; 35 min, 100% B. Solvents A and B were H_2O and CH_3CN 0.1% TFA, respectively. The purified reaction product (2.5 mg) was lyophilized and resuspended in DMSO-d_6 (Cambridge Isotopes) for NMR analysis. Experiments were run on a Bruker 700 MHz spectrometer (Center for Microbial Chemical Biology, McMaster University) to determine the position of the deuterium.

Purification and NMR analysis of ^{13}C-serine reaction products

EdeM assays were carried out in 1 mL reactions containing 100 mM HEPES [pH 7.5], 150 mM NaCl, 150 mM of enzyme, and either 1 mg of L-serine-2-^{13}C or L-serine-1-^{13}C. Reactions were incubated at 30°C for

1 h before derivatizing the reaction contents with Marfey's reagent, as previously described. The derivatized samples were then lyophilized and resuspended in 1 mL of DMSO before loading the entire volume onto a 4.3 g C18 RediSep column for purification via flash chromatography (CombiFlash Rf 200) (solvent A: H_2O 0.1% formic acid, solvent B: CH_3CN -). This method separated the ^{13}C-labelled starting material and the ^{13}C-labelled D-β-serine reaction product. No-enzyme control reactions containing 1 mg of L-serine-2-^{13}C or L-serine-1-^{13}C were also prepared and purified using the same methods. The purified controls and ^{13}C-labelled D-β-serine reaction product were lyophilized and resuspended in DMSO-d_6 (Cambridge Isotopes) for NMR. Experiments were run on a Bruker 700 MHz spectrometer (Center for Microbial Chemical Biology, McMaster University) to determine the position of the D-β-serine ^{13}C labels.

Edeine Purification

Starter cultures of B. brevis Vm4 were grown in a 500 mL baffled Erlenmeyer flask containing 100 mL of PY media (in 1L ddH_2O: 10 g peptone from casein, 5 g yeast extract, 5 g NaCl, and after autoclaving, add $MgCl_2$ 50 mg/mL and $MnCl_2$ 30 mg/mL) at 30°C for 3 days at 250 rpm. The starter culture was used to inoculate 4L (1:50 inoculum) of yeast minimal media (in 1L ddH_2O: 15 g glycerol, 15 g yeast extract, 1.5 g $CaCO_3$, 10 mL of precursor solution 1 [in 50 mL ddH_2O: 200 mg each of arginine, ornithine, lysine, glutamic acid, phosphor-serine, serine, and glycine] and solution 2 [in 50 mL ddH_2O: 200 mg each of tyrosine and phenylalanine, pH adjusted to pH 8.0 with NaOH]). The bulk culture was pH-adjusted to pH 7.0 and aliquoted into 50 mL volumes in separate 250 mL baffled Erlenmeyer flasks. Flasks were incubated at 30°C overnight at 250 rpm. Following incubation, cells were harvested by centrifugation at 6,400 × g and the supernatant was combined with 5% v:v (wet) HP20 resin and incubated overnight at 4°C with gentle rocking. Compounds were extracted from the resin via batch extraction using a MeOH:ddH_2O 20% v:v stepwise gradient from 0-100% MeOH (20, 40, 60, 80, 100% MeOH fractions), with a 4X volume-to-resin ratio for each fraction. Fractions were tested for edeine activity via Kirby-Bauer disk diffusion assays against E. coli BW25113 Δ*bamB* Δ*tolC* (control, edeine^s) and E. coli BW25113 Δb*amB* Δ*tolC* pGDP1:*edeQ* (test strain, edeine^r) on LB agar Petri dishes by spotting 20 mL of each fraction onto 6 mm thick antibiotic test disks (A.M.D. Manufacturing Inc). The 40, 60, and 80% fractions were found to possess activity against the edeine^s strain but not the edeine^r strain, indicating the presence of edeine. Active fractions were pooled, lyophilized, and resuspended in 200 mL of ddH_2O. Resuspended active fractions were next combined with preconditioned AG 50-X4 resin (20 mL of hydrated resin was washed with three 10X volumes of ddH_2O) (hydrogen-form, 50–100 mesh, Bio-Rad and gently agitated for 30 minutes at room temperature. The resin was applied into a glass column (2.5 x 25 cm) and washed with an additional 5X column volume of ddH_2O. A 0.1-1 M gradient of NH_4OH was used to elute edeine from the column. Following elution, the resin was washed with an additional 3X column volume of NH_4OH to remove any remaining edeine from the column. Fractions (10 mL) were collected throughout the elution and neutralized to pH 7.0 through dropwise titration of glacial acetic acid. Fractions were tested for antibiotic activity; positive fractions were pooled and lyophilized before the final purification step using a

Sephadex G-50 size-exclusion column (2.8 x 90 cm) in water at a flow rate of 60 mL/hour. Fractions (6 mL) were assessed for antibiotic activity, and the active fractions were lyophilized. The presence of edeine B was confirmed via 700 MHz NMR (^{1}H, ^{13}C, COSY, HSQC, HMBC (Bruker AVIII)) and LC-MS (Agilent 6546 Q-ToF with a dual AJS electrospray ionization source). A total of 70 mg of edeine was obtained from 4 L of B. brevis Vm4 culture.

Edeine Hydrolysis and Mass Spectroscopy

Purified edeine B was hydrolyzed by combining 2.6 mg of sample with 5 mL of 6N HCl and incubating the mixture at 90°C for 24 h before evaporation under a stream of N_2. The hydrolyzed edeine sample was derivatized with Marfey's reagent as previously described. Samples were injected on the Q-TOF LC/MS (Agilent Technologies 6550 iFunnel) using an Agilent Eclipse XDB-C8 column (3.5 µm, 2.1 x 100 mm. The LC/MS was run at 0.2 mL/min using the following gradient: 1 min, 5% B; 7 min, 95% B; 7.5 min, 95% B; 8 min, 95% B. Solvents A and B were 0.1% formic acid in H_2O and CH_3CN, respectively.

Computational chemistry

Density Functional Theory (DFT) calculations were performed using the Gaussian 16, Revision C. 01 program[39]. Optimizations were conducted using the Head-Gordon's range-separated hybrid ωB97X-D functional[40] with Pople type basis sets placing diffuse and polarization functions on all atoms. This functional was selected as it accounts for dispersion and has been shown to provide accurate thermochemical and kinetic energies. Further the default parameter of the Gaussian 16 program was used. All optimizations were carried out in solvent at the $SMD_{(H2O)}$ωB97X-D/6–31 + G(d,p) level of theory[41]. Frequency calculations were carried out at the same level of theory as that used for geometry optimization to characterize the stationary points as either minima (no imaginary frequencies) or first order saddle points, i.e., transition states (one imaginary frequency) on the potential energy surface. The keyword (integral=grid=ultrafine) was used for all calculations. The 3D molecular visualizations were created using CYLview[42]. GaussView 6.1[43] was used to construct all structures prior to optimization and to visualize the output from the Gaussian 16 program calculations. The reported ESP surface of **TS-1** in Fig. 7 was obtained from the Jaguar program[44, 45] of the Schrödinger software package.

Declarations

Competing interest

The authors declare no competing interest.

Ethics declaration

Not applicable.

Funding

This work was supported by funding from the Natural Sciences and Engineering Council of Canada Discovery Grant to G.D.W (RGPIN-2024-06372) and the Natural Sciences and Engineering Research Council of Canada Alexander Graham Bell Canada Graduate Scholarship-Doctoral to H.L.Z (CGSD3–547411 – 2020). A.B. is supported by The Swedish Foundation for International Cooperation in Research and Higher Education (STINT) and the Swedish Pharmaceutical Society (Elisabeth & Alfred Ahlqvists stiftelse) Postdoctoral fellowships. Crystallography studies described in this paper were performed using beamline CMCF-ID at the Canadian Light Source, a national research facility of the University of Saskatchewan, which is supported by the Canada Foundation for Innovation (CFI), the Natural Sciences and Engineering Research Council (NSERC), the National Research Council (NRC), the Canadian Institutes of Health Research (CIHR), the Government of Saskatchewan, and the University of Saskatchewan. The authors gratefully acknowledge the Centre for Microbial Chemical Biology (CMCB) and the McMaster Macromolecular X-ray diffraction facility for instrumentation and support. T.D. thanks the Natural Sciences and Engineering Research Council of Canada for Discovery Grants (RGPIN-2025-04511) and NSERC Alliance International Collaboration Grant (ALLRP 606966–25). Computations were carried out using facilities at Digital Research Alliance of Canada; this research was enabled in part by support provided by SHARCNET (Shared Hierarchical Academic Research Computing Network) and Compute/ Calcul Canada and the Digital Research Alliance of Canada.

Author contributions

A.B. and H.L.Z designed and carried out the majority of the experiments, conducted the mechanistic investigations, and drafted and wrote the manuscript. K.K. performed NMR-experiments, contributed to QtoF mass spectrometry analysis and wrote the manuscript. E.V.M. carried out protein production and purification. B.W. and T.D. performed the computational studies and wrote the manuscript. J.P.W. purified edeine. E.L.W. carried out molecular cloning. S.N.A. performed the crystallographic studies and wrote the manuscript. G.D.W. conceived the study, supervised the work and wrote the manuscript.

Acknowledgements

We are very thankful for the kind gift of the *Breviacillus brevis* Vm4 strain from Dr. Zofia Kurylo-Borowska. We thank Dr. Gang Wu for kindly providing ^{17}O-3-L-serine for the isotope labeling studies of β-serine biosynthesis. We thank Amna Abbas for help with protein purification and Dr. Peter Brandt, Dr. Lindon Moodie and Dr. Jakob Magolan for helpful discussions.

Data Availability

The data supporting the findings of this study are available within the article and its Supplementary Information. The crystallographic data have been deposited in the Protein Data Bank under accession codes (38RJ and 38JZ). Raw data supporting the findings are provided with this paper. Additional data are available from the corresponding author upon reasonable request.

References

1. Patočka J (2011) β-amino acids and their natural biologically active derivatives. Mil Med Sci Lett 80:2–11
2. Walsh CT, O'Brien RV, Khosla C (2013) Nonproteinogenic amino acid building blocks for nonribosomal peptide and hybrid polyketide scaffolds. Angew Chem Int Ed Engl 52:7098–7124
3. Kudo F, Miyanaga A, Eguchi T (2014) Biosynthesis of natural products containing beta-amino acids. Nat Prod Rep 31:1056–1073
4. Turner NJ (2011) Ammonia lyases and aminomutases as biocatalysts for the synthesis of alpha-amino and beta-amino acids. Curr Opin Chem Biol 15:234–240
5. Safdari HA et al (2025) The translation inhibitors kasugamycin, edeine and GE81112 target distinct steps during 30S initiation complex formation. Nat Commun 16:2470
6. Kurylo-Borowska Z (1959) Isolation and properties of pure edeine, an antibiotic of the strain Bacillus brevis Vm4. Biul Inst Med Morsk Gdansk 10:151–163
7. Kurylo-Borowska Z (1975) Biosynthesis of edeine: II. Localization of edeine synthetase within Bacillus brevis Vm4. Biochim Biophys Acta 399:31–41
8. Westman EL, Yan M, Waglechner N, Koteva K, Wright GD (2013) Self resistance to the atypical cationic antimicrobial peptide edeine of Brevibacillus brevis Vm4 by the N-acetyltransferase EdeQ. Chem Biol 20:983–990
9. Kurylo-Borowska Z, Abramsky T (1972) Biosynthesis of β-tyrosine. Biochim Biophys Acta 264:1–10
10. Beasley FC, Cheung J, Heinrichs DE (2011) Mutation of L-2,3-diaminopropionic acid synthase genes blocks staphyloferrin B synthesis in Staphylococcus aureus. BMC Microbiol 11:199
11. Kobylarz MJ et al (2014) Synthesis of L-2,3-diaminopropionic acid, a siderophore and antibiotic precursor. Chem Biol 21:379–388
12. Du YL, Ryan KS (2019) Pyridoxal phosphate-dependent reactions in the biosynthesis of natural products. Nat Prod Rep 36:430–457
13. Daniel-Ivad P, Ryan KS (2024) New reactions by pyridoxal phosphate-dependent enzymes. Curr Opin Chem Biol 81:102472
14. Phillips RS (2015) Chemistry and diversity of pyridoxal-5'-phosphate dependent enzymes. Biochim Biophys Acta 1854:1167–1174

15. Zhang Z et al (2025) NRPStransformer, an Accurate Adenylation Domain Specificity Prediction Algorithm for Genome Mining of Nonribosomal Peptides. J Am Chem Soc 147:32662–32670
16. Terlouw BR et al (2026) High-Accuracy Machine Learning of Substrate Specificities in Nonribosomal Peptide Synthetases. JACS Au 6:2315–2336
17. Volpe MR et al (2023) A small molecule inhibitor prevents gut bacterial genotoxin production. Nat Chem Biol 19:159–167
18. Kirsch JF et al (1984) Mechanism of action of aspartate aminotransferase proposed on the basis of its spatial structure. J Mol Biol 174:497–525
19. Bar-Even A et al (2011) The moderately efficient enzyme: evolutionary and physicochemical trends shaping enzyme parameters. Biochemistry 50:4402–4410
20. Toney MD, Kirsch JF (1991) Tyrosine 70 fine-tunes the catalytic efficiency of aspartate aminotransferase. Biochemistry 30:7456–7461
21. Graber R et al (1995) Changing the reaction specificity of a pyridoxal-5'-phosphate-dependent enzyme. Eur J Biochem 232:686–690
22. Markova M, Peneff C, Hewlins MJ, Schirmer T, John RA (2005) Determinants of substrate specificity in omega-aminotransferases. J Biol Chem 280:36409–36416
23. Walsh CT (1979) *Enzymatic Reaction Mechanisms*, Edn. 1st. (W. H. Freeman & Co, San Francisco
24. Braunstein AE (1964) Binding and Reactions of the Vitamin B6 Coenzyme in the Catalytic Center of Aspartate Transaminase. Vitam Horm 22:451–484
25. Toney MD (2014) Aspartate aminotransferase: an old dog teaches new tricks. Arch Biochem Biophys 544:119–127
26. Quast H, Schmitt E, Frank R (2003) Cyclopropanimines. A Novel Variant of the Favorskii Reaction. Angewandte Chemie Int Ed Engl 10:651–652
27. Baldwin J (1978) Rules for ring closure. Ciba Found Symp, 85–99
28. Alabugin IV, Gilmore K (2013) Finding the right path: Baldwin rules for ring closure and stereoelectronic control of cyclizations. Chem Commun (Camb) 49:11246–11250
29. Moens the favorskii-rearrangement of alpha-chloro-ketimines (2002)
30. Wiering PG, Steinberg H (2013) Rearrangements of Methyl Substituted N-Neopentylmethyleneaziridines in Methanol. Isr J Chem 22:56–58
31. Quast H, Fuss A, Heublein A, Jakobi H, Seiferling B (1991) Photochemical Formation of Heteromethylenecyclopropanes.24. Retention of Configuration in 2 Photochemical-Reactions - Formation of Cyclopropanimines by Extrusion of Molecular Nitrogen from Tetraalkyl-4-Imino-1-Pyrazolines and [2 + 1] Cycloreversion of Cyclopropanimines to Isocyanides and Alkenes. Chem Ber 124:2545–2554
32. Grochulski P, Fodje MN, Gorin J, Labiuk SL, Berg R (2011) Beamline 08ID-1, the prime beamline of the Canadian Macromolecular Crystallography Facility. J Synchrotron Radiat 18:681–684

33. Emsley P, Lohkamp B, Scott WG, Cowtan K (2010) Features and development of Coot. Acta Crystallogr D Biol Crystallogr 66:486–501
34. Liebschner D et al (2019) Macromolecular structure determination using X-rays, neutrons and electrons: recent developments in Phenix. Acta Crystallogr D Struct Biol 75:861–877
35. Abramson J et al (2024) Accurate structure prediction of biomolecular interactions with AlphaFold 3. Nature 630:493–500
36. Chen X et al (2025) Protenix - Advancing Structure Prediction Through a Comprehensive AlphaFold3 Reproduction. *bioRxiv*
37. PyMOL Molecular Graphics System. Version 3.1.4.1 (2025)
38. King AM et al (2014) Aspergillomarasmine A overcomes metallo-beta-lactamase antibiotic resistance. Nature 510:503–506
39. Frisch MJ et al (2016) (Wallingford, CT
40. Chai JD, Head-Gordon M (2008) Long-range corrected hybrid density functionals with damped atom-atom dispersion corrections. Phys Chem Chem Phys 10:6615–6620
41. Marenich AV, Cramer CJ, Truhlar DG (2009) Universal solvation model based on solute electron density and on a continuum model of the solvent defined by the bulk dielectric constant and atomic surface tensions. J Phys Chem B 113:6378–6396
42. Legault CV (2009) Edn. 1.0b. Universite de Sherbrooke, Quebec, Canada
43. Dennington RK, T. A. and, Milliam JM (2016) (Shawnee Mission, Semichem Inc
44. Bochevarov AD et al (2013) A high-performance quantum chemistry software program with strengths in life and materials sciences. Int J Quantum Chem 113:2110–2142Jaguar
45. Schrödinger E (2024) New York, USA;. Jaguar, Release 2025-1

Figures

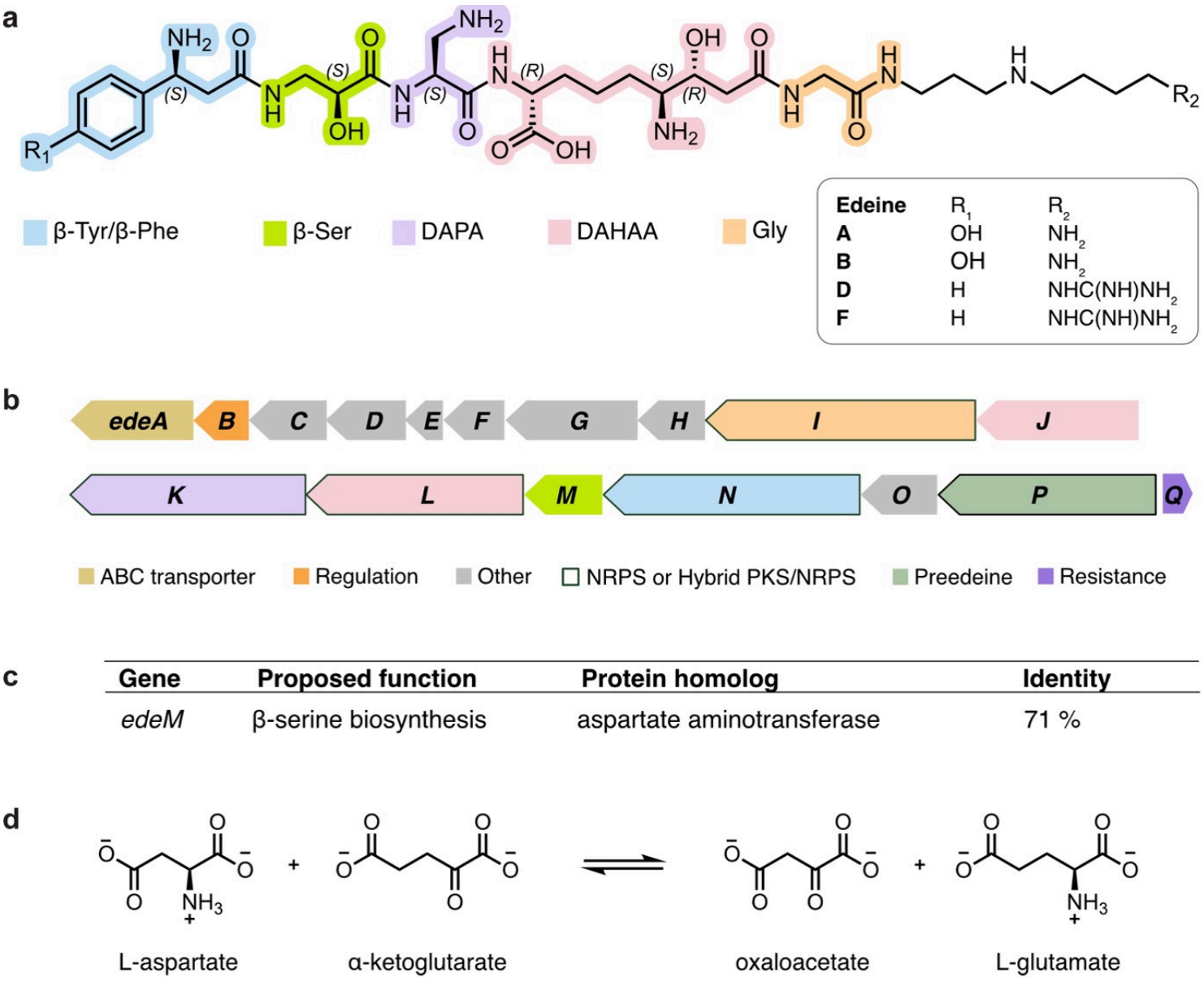

c

Gene	Proposed function	Protein homolog	Identity
edeM	β-serine biosynthesis	aspartate aminotransferase	71 %

Figure 1

EdeM encodes a putative β-serine synthase. a. The antibiotics edeines contains four nonproteinogenic amino acids, including three β-amino acids: β-tyrosine/β-phenylalanine, β-serine, and 2,3-diaminopropionic acid (DAPA), as well as the gamma-amino acid 2,6-diamino-7-hydroxyazelaic acid (DAHAA). **b**. The edeine biosynthetic gene cluster (45.1 kb). **c**. The closest protein homolog for EdeM is aspartate aminotransferase, which belongs to a family of pyridoxal 5' phosphate-dependant enzymes known as transaminases, which can transfer amino groups between substrates. **d**. The aspartate aminotransferase reaction requires two substrates, L-aspartate and α-ketoglutarate, and is catalyzed by PLP to form oxaloacetate and L-glutamate.

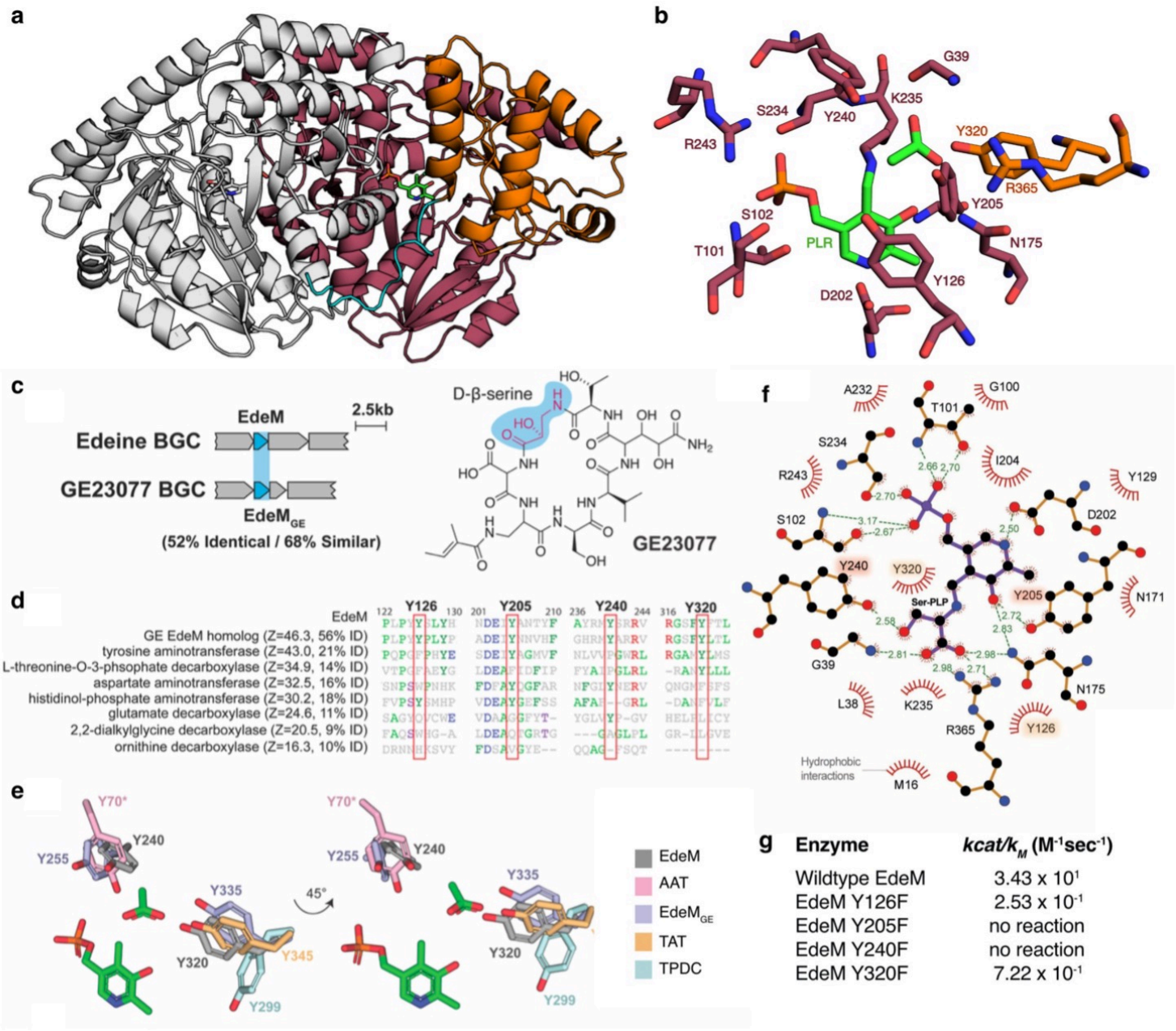

Figure 2

Active-site tyrosine residues drive EdeM-catalyzed D-β-serine formation. a, The homodimeric crystal structure of EdeM (PDB: 38RJ, 2.3 Å) in complex with reduced PLP (PLR) and acetate depicted as green sticks. The large PLP-binding domain is shown in maroon, the small flexible domain in orange and the short N-terminal strand in cyan. **b,** Close-up of the active site residues (maroon sticks) around PLR and acetate (green sticks). **c**, The antibiotic GE23077 (GE) contains D-β-serine. Alignment of the GE BGC and the edeine BGC revealed a potential EdeM homolog, GE-EdeM. **d,** Structural alignments were conducted with EdeM (2.3 Å) against an AlphaFold 3 model of GE-EdeM (pTM: 0.92, ipTM: 0.0), tyrosine aminotransferase [PDB 1BW0, 2.50 Å], L-threonine-O-3-phosphate decarboxylase [1LKC, 1.80 Å], aspartate aminotransferase [1ARG, 2.20 Å], histidinol-phosphate aminotransferase [4RAE, 2.59 Å], glutamate decarboxylase [5GP4, 2.16 Å], 2,2,-dialkylglycine decarboxylase [1M0N, 2.20 Å], and ornithine

decarboxylase [1ORD, 3.00 Å]. Results for Y126, Y205, Y240, and Y320 based on EdeM numbering are outlined in red. **e,** Overlay of selected tyrosine residues from EdeM (gray), aspartate aminotransferase (AAT) (pink), GE-EdeM (purple), tyrosine aminotransferase (TAT) (orange), L-threonine-O-3-phosphate decarboxylase (TPDC) (blue). PLR and acetate from the EdeM crystal structure are shown in green. **f,**A ligplot 2D analysis of L-ser-PLP in EdeM showing hydrogen bond lengths (Å) in green and hydrophobic interactions as red halos. Key tyrosine residues Y240 and Y205 making hydrogen bonds with Ser-PLP highlighted in red. **g,** Catalytic efficiency of EdeM showing the specificity constants of wildtype EdeM and EdeM Tyr-to-Phe active-site mutants.

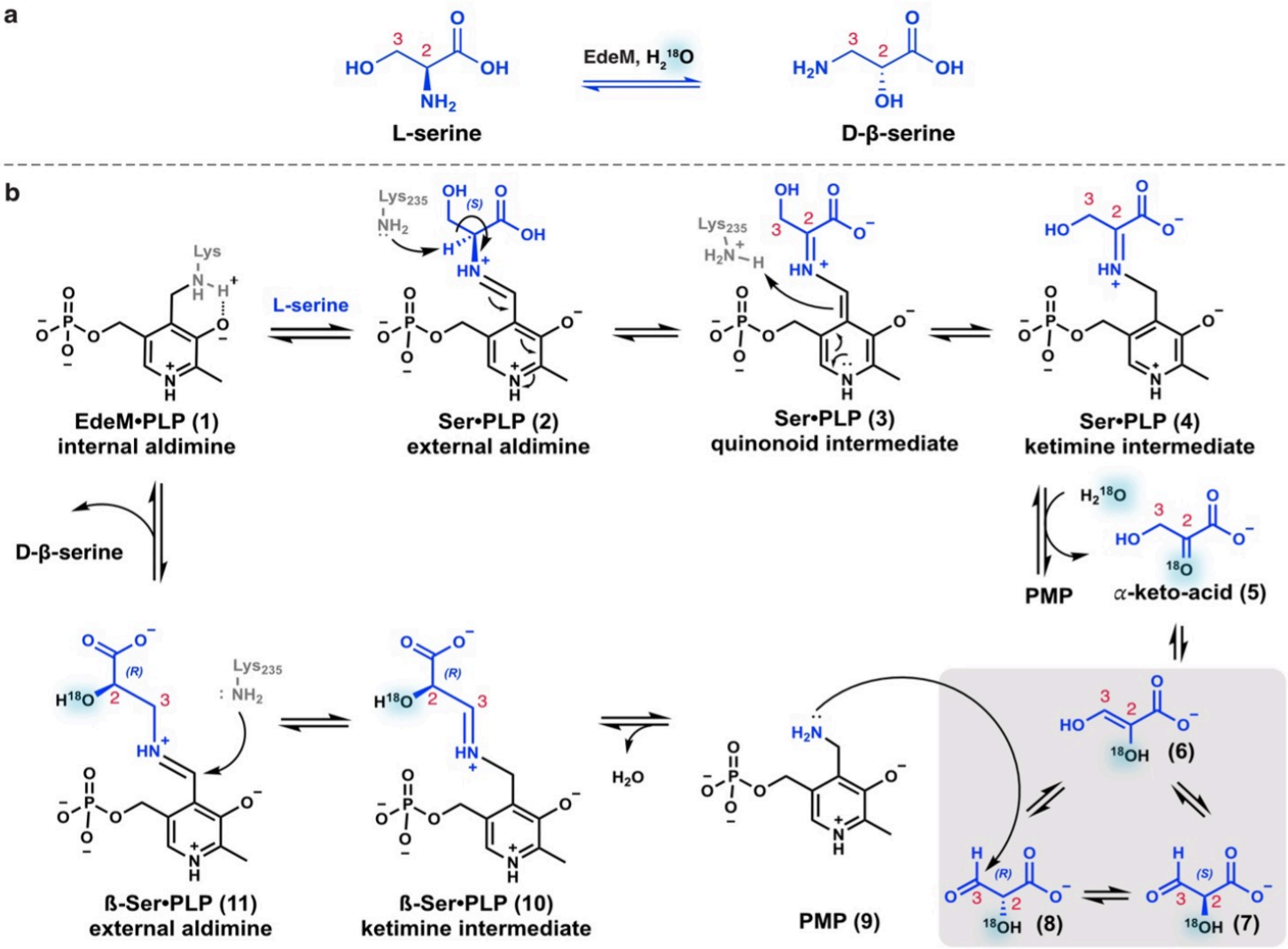

Figure 3

Transaminase-like two half-reaction mechanism is incompatible with EdeM isotope-labeling results. a, The enzymatic reaction was conducted in $H_2{}^{18}O$ and the product analysed. **b**, Proposed reaction mechanism. The predicted ^{18}O incorporation expected from hydrolysis in the first half-reaction was not observed in the product. Isotopic labeling and NMR analysis of the product shows that carbons two and

three (marked in red) swap places. These results indicate that EdeM does not operate via a classical PLP transamination cycle.

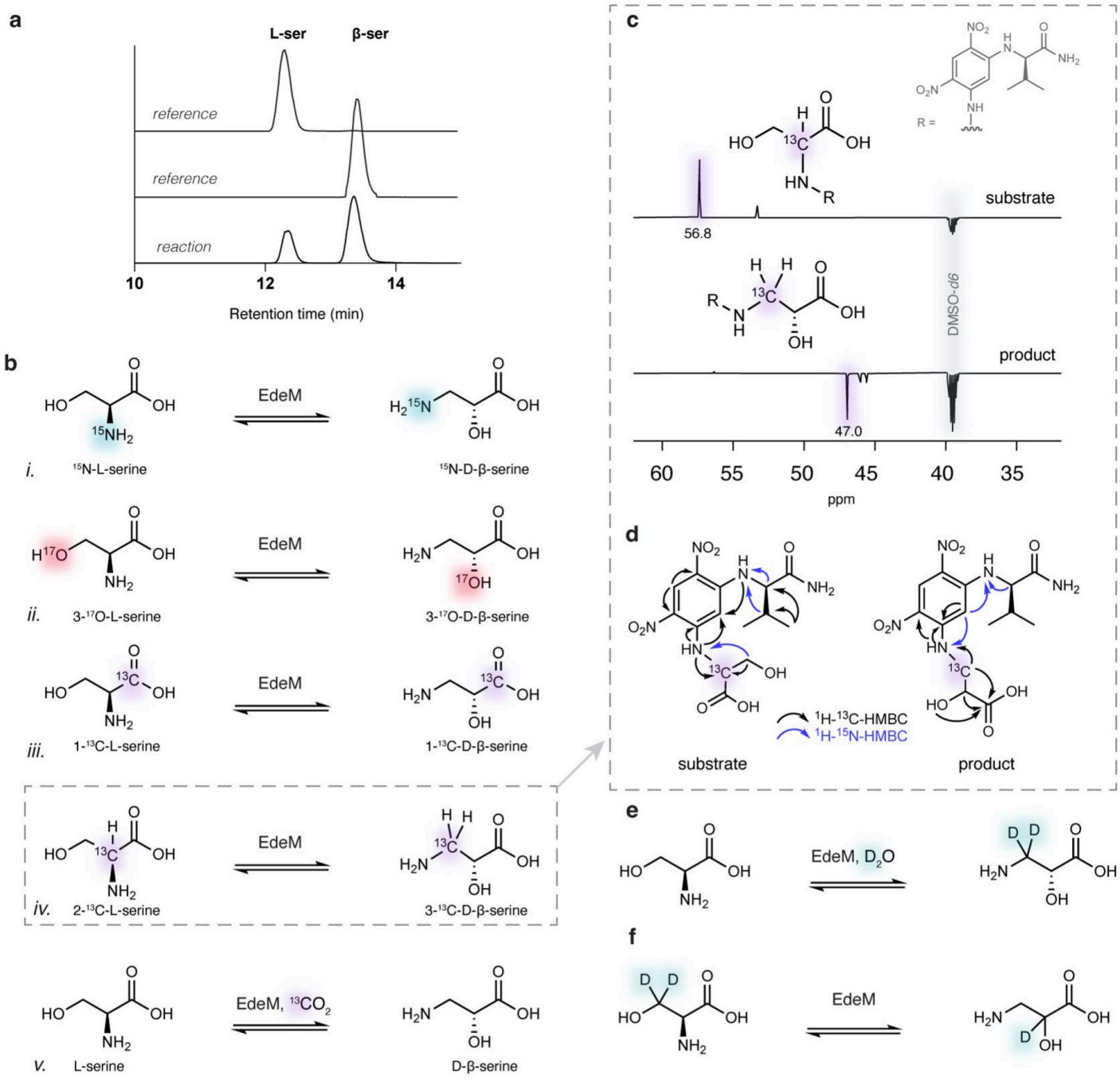

Figure 4

Stable isotope investigation reveals an EdeM-catalyzed intramolecular rearrangement. a, Positive mode extracted ion chromatogram (+EIC) at 386.13 *m/z*. Standards for Marfey's derivatized L-serine (12.5 min) and D-β-serine (13.5 min) are shown as reference, with 1-hour EdeM reaction on the bottom after derivatization. While the peak for L-serine is present, there is also the formation of a second peak that corresponds with D-β-serine. **b**, ^{15}N (*i*), ^{17}O (*ii*), 1-^{13}C (*iii*) and 2-^{13}C (*iv*) are retained in the product

after a 1-hour EdeM reaction. $^{13}CO_2$ (*v*) is not incorporated into the product after a 1-hour EdeM reaction. **c**, ^{13}C-NMR DEPTQ-135 spectra reveal that substrate 2-^{13}C-L-serine becomes 3-^{13}C-D-β-serine, showing a positive phase for the 2-CH carbon before the reaction and then, after the EdeM reaction, the labelled carbon has become a 3-CH_2 carbon, as seen with a negative phase peak. **d**, The structures were further confirmed by ^{1}H-^{13}C- HMBC (black arrow) and ^{1}H-^{15}N-HMBC (blue arrow) interactions. **e**, L-serine reaction with EdeM in D_2O shows incorporation of two atoms of deuterium (Δm = +2 Da) into D-β-serine **f**, L-3,3-D_2-serine reacted with EdeM results in 2-D_1-β-serine.

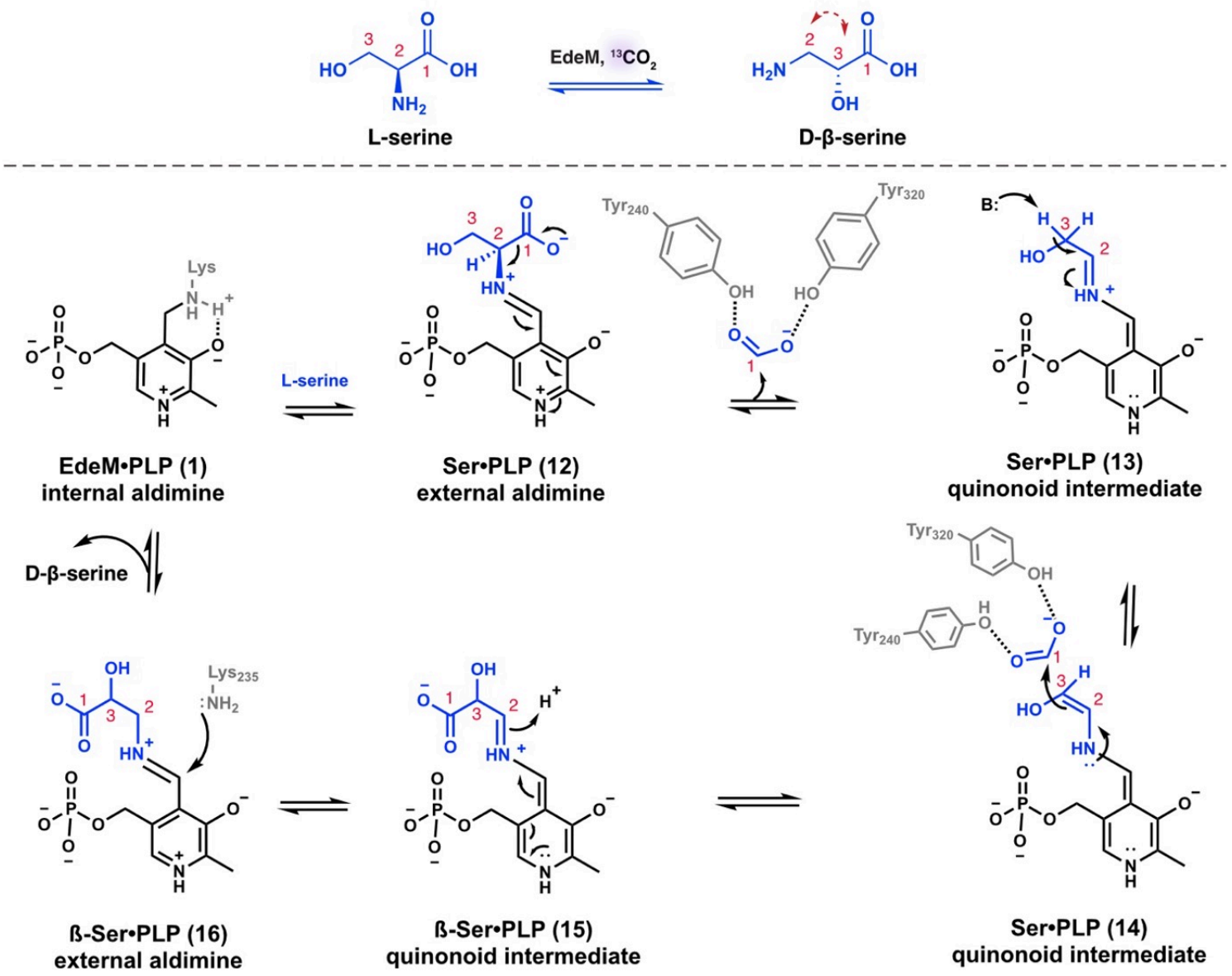

Figure 5

Proposed rearrangement mechanism of CO_2 through decarboxylation. $^{13}CO_2$ exchange experiment following degassing and gas replacement shows no ^{13}C incorporation into D-β-serine, indicating that exogenous CO_2 is not incorporated during the rearrangement.

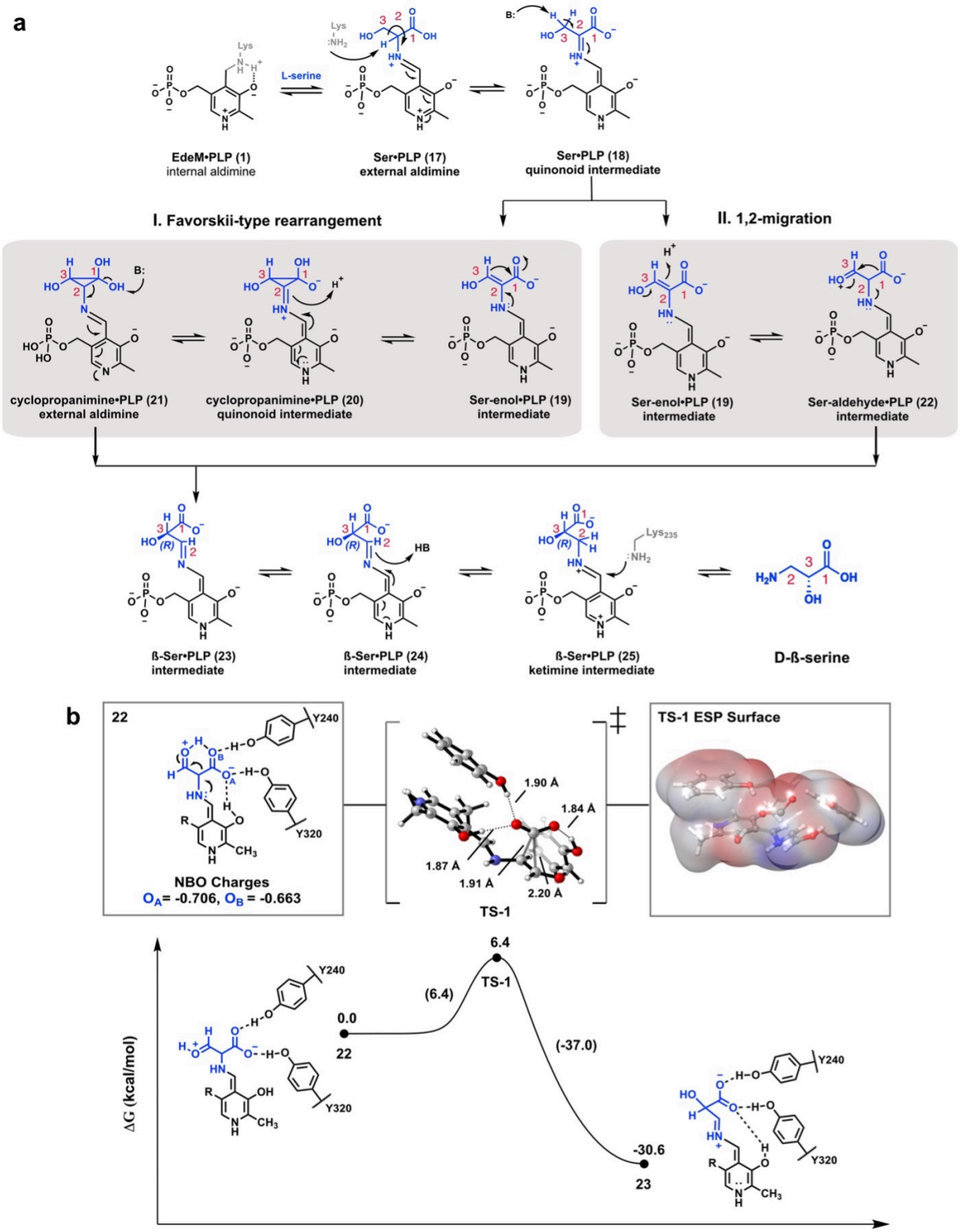

Figure 6

Proposed rearrangement mechanisms of EdeM-catalyzed D-b-serine formation and computational support for 1,2-migration pathway**. a, I. A Favorskii-type mechanism via 3-exo-trig closure and cyclopropanimine intermediate or II. A 1,2-migration pathway, resulting in the corresponding** D-b-serine product. **b**, Free energy profile for the concerted 1,2-carboxylate migration from **22** through TS-1 to **23**,

with key bond distances and NBO charges shown. Free energies were calculated at the SMD(H_2O)/ωB97X-D/6-31+G(d,p) level of theory.

Supplementary Files

This is a list of supplementary files associated with this preprint. Click to download.

- EdeMSupportingInformation.pdf
- Graphicalabstract.png